

Uhlmann Phase Winding in Bose-Einstein Condensates at Finite Temperature

Chang-Yan Wang*

Institute for Advanced Study, Tsinghua University, Beijing 100084, China

Yan He†

College of Physics, Sichuan University, Chengdu, Sichuan 610064, China

We investigate the Uhlmann phase, a generalization of the celebrated Berry phase, for Bose-Einstein condensates (BECs) at finite temperature. The Uhlmann phase characterizes topological properties of mixed states, in contrast to the Berry phase which is defined for pure states at zero temperature. Using the $SU(1,1)$ symmetry of the Bogoliubov Hamiltonian, we derive a general formula for the Uhlmann phase of BECs. Numerical calculations reveal that the Uhlmann phase can differ from the Berry phase in the zero-temperature limit, contrary to previous studies. As the temperature increases, the Uhlmann phase exhibits a winding behavior, and we relate the total winding degree to the Berry phase. This winding indicates that the Uhlmann phase takes values on a Riemann surface. Furthermore, we propose an experimental scheme to measure the Uhlmann phase of BECs by purifying the density matrix using an atomic interferometer.

I. INTRODUCTION

The Berry phase [1, 2], acquired by a quantum system undergoing an adiabatic evolution, can characterize the topological properties of quantum systems at zero temperature, such as the quantum Hall effect [3]. However, Berry phase is only defined for pure states, while in reality, most quantum systems are in contact with an environment, existing at finite temperatures and consequently described by mixed states. To bridge this gap, the Uhlmann phase was introduced, extending the concept of geometric phase to mixed states through the adiabatic evolution of density matrix [4–7].

The Uhlmann phase has been the subject of extensive studies for mixed states [8–13], and has recently attracted considerable attention for investigating the topological properties of various quantum systems at finite temperatures [14–25], including fermionic lattice models [26–28] and spin systems [29–31]. Despite this, the Uhlmann phase for Bose-Einstein condensates (BECs)—one of the most important states of matter in ultracold atomic systems—has not been explored. Given the high controllability of BEC systems [32], the study of the Uhlmann phase of BEC can enrich our understanding of topological properties at finite temperatures and for mixed states.

In this paper, we study the Uhlmann phase of BEC by exploiting the so-called $SU(1,1)$ symmetry of the Bogoliubov Hamiltonian. The $SU(1,1)$ group, a non-compact Lie group, includes the transformations preserving the canonical commutation relation of bosonic operators of BEC [33]. This group has been widely used in quantum optics [34, 35], and recently finds its application in studying the dynamics and quantum echo of BEC [36–41]. Meanwhile, the similar symmetric approach has been generalized to two-component BEC [42–46].

By using the $SU(1,1)$ symmetry, the density matrix of the BEC at finite temperature can be parameterized as a Poincare disk, akin to the Bloch sphere for the spin system. The adiabatic Uhlmann process is then represented by a trajectory within this disk. By considering different paths, we find that the Uhlmann phase of BEC can differ from the zero-temperature Berry phase, contrary to previous studies on the Uhlmann phase. Meanwhile, we find that the Uhlmann phase of BEC displays a unique winding behavior when the temperature increases from low to high. More interestingly, the total winding degree is equal to the negative of the Berry phase at zero temperature. This winding behavior indicates that the Uhlmann phase takes values in a Riemann surface. We further propose a scheme to measure the Uhlmann phase of BEC experimentally based on purification of the density matrix using an atomic interferometer which uses the interference of atoms to perform precise measurements [47].

Our work highlights the systematic use of the non-trivial $SU(1,1)$ symmetry of BEC and unveil a novel Uhlmann phase winding feature previously unreported. This winding behavior establishes an interesting link between the geometric phase behaviors at zero and finite temperatures. Moreover, our study also relates this winding behavior to the geometric nature of the Uhlmann phase by demonstrating its association with a curve in Riemann surface.

The rest of this paper is organized as follows: in Sec. II, we review Bogoliubov Hamiltonian of BEC and its $SU(1,1)$ symmetry; in Sec. III, we briefly review the definition of Uhlmann phase; in Sec. IV, we derive the Uhlmann phase of BEC, and present the general method to numerically calculate the Uhlmann phase of BEC; in Sec. V, we present the numerical results, and reveal the Uhlmann phase winding; in Sec. VI, we discuss how to observe the Uhlmann phase of BEC experimentally; we conclude in Sec. VII.

* changyanwang@tsinghua.edu.cn

† heyan.ctp@scu.edu.cn

II. BEC HAMILTONIAN AND $SU(1,1)$ SYMMETRY

We consider an interacting bosonic gas, the Hamiltonian of which in momentum space can be written as

$$\hat{H} = \sum_{\mathbf{k}} \epsilon_{\mathbf{k}} a_{\mathbf{k}}^{\dagger} a_{\mathbf{k}} + \frac{g}{2V} \sum_{\mathbf{k}, \mathbf{k}', \mathbf{q}} a_{\mathbf{k}+\mathbf{q}}^{\dagger} a_{\mathbf{k}'-\mathbf{q}}^{\dagger} a_{\mathbf{k}'} a_{\mathbf{k}}, \quad (1)$$

where $a_{\mathbf{k}} (a_{\mathbf{k}}^{\dagger})$ is the annihilation (creation) operator for bosons with momentum \mathbf{k} , and $\epsilon_{\mathbf{k}} = \mathbf{k}^2/2m - \mu$, $g = 4\pi\hbar^2 a_s/m$, with a_s the s-wave scattering length, which can be tuned through Feshbach resonance [32]. In the following we will set $\hbar = 1$ for simplicity.

Due to Bose-Einstein condensation, most bosons will stay at the lowest energy state with $\mathbf{k} = 0$. Making use of the Bogoliubov approximation, we can expand the interaction terms around the condensate up to the quadratic terms of boson operators. Then we arrive at the Bogoliubov Hamiltonian of BEC as follows $\hat{H}_{\text{Bog.}} = \sum_{\mathbf{k} \neq 0} \hat{H}_{\mathbf{k}} + \text{const.}$, where

$$\hat{H}_{\mathbf{k}} = \sum_{i=0}^2 \xi_i(\mathbf{k}) K_i. \quad (2)$$

Here, the coefficients are $\xi_0 = 2(\epsilon_{\mathbf{k}} + g|\Psi_0|^2)$, $\xi_1 = 2\text{Re}(g\Psi_0^2)$, $\xi_2 = -2\text{Im}(g\Psi_0^2)$ and $\Psi_0 = \sqrt{N_0/V} e^{i\theta}$ is the condensate wavefunction. The operators in Eq.(2) are defined as

$$\begin{aligned} K_0 &= \frac{1}{2}(a_{\mathbf{k}}^{\dagger} a_{\mathbf{k}} + a_{-\mathbf{k}} a_{-\mathbf{k}}^{\dagger}), \\ K_1 &= \frac{1}{2}(a_{\mathbf{k}}^{\dagger} a_{-\mathbf{k}}^{\dagger} + a_{\mathbf{k}} a_{-\mathbf{k}}), \\ K_2 &= \frac{1}{2i}(a_{\mathbf{k}}^{\dagger} a_{-\mathbf{k}}^{\dagger} - a_{\mathbf{k}} a_{-\mathbf{k}}), \end{aligned} \quad (3)$$

They are the three generators of $\mathfrak{su}(1,1)$ Lie algebra [34, 39], which satisfy the $\mathfrak{su}(1,1)$ Lie algebra commutation relation

$$[K_0, K_1] = iK_2, [K_2, K_0] = iK_1, [K_1, K_2] = -iK_0. \quad (4)$$

Since the Bogoliubov Hamiltonian $\hat{H}_{\text{Bog.}}$ is decoupled for different momenta, in the following we will focus on the Hamiltonian $\hat{H}_{\mathbf{k}}$ in Eq.(2). This Hamiltonian can be diagonalized by the Bogoliubov transformation, which introduces the quasi-particle excitations as follows

$$\hat{a}_{\mathbf{k}} = u_{\mathbf{k}} a_{\mathbf{k}} + v_{\mathbf{k}} a_{-\mathbf{k}}^{\dagger}, \quad \hat{a}_{-\mathbf{k}} = u_{\mathbf{k}} a_{-\mathbf{k}} + v_{\mathbf{k}} a_{\mathbf{k}}^{\dagger}, \quad (5)$$

where the coefficients $u_{\mathbf{k}}, v_{\mathbf{k}}$ satisfy the condition

$$|u_{\mathbf{k}}|^2 - |v_{\mathbf{k}}|^2 = 1. \quad (6)$$

In terms of quasi-particle operators, the Hamiltonian $\hat{H}_{\mathbf{k}}$ can be diagonalized as $\hat{H}_{\mathbf{k}} = \varepsilon_{\mathbf{k}}(\hat{a}_{\mathbf{k}}^{\dagger} \hat{a}_{\mathbf{k}} + \hat{a}_{-\mathbf{k}}^{\dagger} \hat{a}_{-\mathbf{k}}) + \text{const.}$ with the quasi-particle energy $\varepsilon_{\mathbf{k}} = \sqrt{\xi_0(\mathbf{k})^2 - \xi_1(\mathbf{k})^2 - \xi_2(\mathbf{k})^2}/2$.

In order to compute the Uhlmann phase later, we also need to work out the explicit form of all eigenstates. The ground state of the Hamiltonian $\hat{H}_{\mathbf{k}}$ is defined by $\hat{a}_{\mathbf{k}}|G\rangle = \hat{a}_{-\mathbf{k}}|G\rangle = 0$. One can verify that the ground state is just the generalized coherent state of $SU(1,1)$ group [33, 48]

$$|G\rangle = \frac{1}{\sqrt{1-|z|^2}} e^{-z a_{\mathbf{k}}^{\dagger} a_{-\mathbf{k}}^{\dagger}} |0\rangle, \quad (7)$$

where $z = v_{\mathbf{k}}/u_{\mathbf{k}}$, and $|0\rangle$ is the bare vacuum state. Due to Eq.(6), the norm of z is smaller than 1, i.e. $1-|z|^2 > 0$. Therefore, for all the possible $\hat{H}_{\mathbf{k}}$, their ground states are parameterized by z defined on a two-dimensional unit disk, which is actually the celebrated Poincare disk [33, 39].

On the other hand, the ground state $|G\rangle$ can also be written as a unitary operator $D(\zeta)$ acting on the vacuum state [33]

$$|G\rangle = D(\zeta)|0\rangle \equiv e^{-\zeta a_{\mathbf{k}}^{\dagger} a_{-\mathbf{k}}^{\dagger} + \zeta^* a_{\mathbf{k}} a_{-\mathbf{k}}} |0\rangle, \quad (8)$$

which will be useful for the calculation of Uhlmann phase. Meanwhile, if we write a point z in the Poincare disk as $z = \tanh \frac{r}{2} e^{i\theta}$ with $r \in [0, \infty)$, $\theta \in [-\pi, \pi)$, then ζ is given as $\zeta = \frac{r}{2} e^{i\theta}$ [49]. With this parameterization of ζ , we can also make the Euler decomposition of the operator $D(\zeta)$ as follows [49]

$$D(\zeta) = e^{i\theta K_0} e^{-ir K_2} e^{-i\theta K_0}, \quad (9)$$

which is also needed when calculating the Uhlmann phase.

With the ground state and the creation operators of quasi-particles, we can obtain the excited state

$$|\Psi_{\mathbf{n}}\rangle = \frac{1}{\sqrt{n_1! n_2!}} (\hat{a}_{\mathbf{k}}^{\dagger})^{n_1} (\hat{a}_{-\mathbf{k}}^{\dagger})^{n_2} |G\rangle, \quad (10)$$

where $\mathbf{n} = (n_1, n_2)$ labels the number of each kind of quasi-particles. Note that the Bogoliubov transformation of Eq.(5) can also be written as [33, 34]

$$D(\zeta)^{\dagger} \hat{a}_{\pm\mathbf{k}}^{\dagger} D(\zeta) = a_{\pm\mathbf{k}}^{\dagger}$$

With this fact, it can be shown that

$$|\Psi_{\mathbf{n}}\rangle = \frac{1}{\sqrt{n_1! n_2!}} D(\zeta) (a_{\mathbf{k}}^{\dagger})^{n_1} (a_{-\mathbf{k}}^{\dagger})^{n_2} |0\rangle = D(\zeta)|\mathbf{n}\rangle, \quad (11)$$

where we have defined

$$|\mathbf{n}\rangle = \frac{1}{\sqrt{n_1! n_2!}} (a_{\mathbf{k}}^{\dagger})^{n_1} (a_{-\mathbf{k}}^{\dagger})^{n_2} |0\rangle. \quad (12)$$

Thus, one can see that the excited states $|\Psi_{\mathbf{n}}\rangle$ are also parameterized by a point z on the Poincare disk. And the eigenenergy of this excited state is given by $E_{\mathbf{n}} = \varepsilon_{\mathbf{k}}(n_1 + n_2)$. Here we have shifted the ground state energy to 0 for simplicity. This shift will not affect the calculation of Uhlmann phase in the following sections.

III. UHLMANN PROCESS AND UHLMANN CONNECTION

The Uhlmann phase is a generalization of the celebrated Berry phase for quantum systems at finite temperature and mixed quantum states [5–7]. In this section, we will briefly review the concept of Uhlmann connection and Uhlmann phase.

When a quantum system undergoes an adiabatic cyclic process in the parameter space, its n -th eigenstate $|\psi_n(t)\rangle$ with $t \in [0, 1]$ parameterizing the adiabatic path on the parameter space, will acquire a phase factor, i.e. $|\psi_n(1)\rangle = e^{i\Phi_B}|\psi_n(0)\rangle$, where Φ_B is the Berry phase. The Berry phase can be obtained by integrating the Berry connection $A_B = -i\langle\psi_n|\frac{d}{dt}|\psi_n\rangle$, i.e. $\Phi_B = \int A_B dt$, as illustrated in Figure 1(a).

For a finite-temperature system or a mixed state, its physical properties can be computed from the density matrix ρ instead of wave functions. One can always make a spectral decomposition of density matrices as $\rho = \sum_i \lambda_i |u_i\rangle\langle u_i|$. Here $|u_i\rangle$ for $i = 1, \dots, n$ are eigenstates and $\lambda_i = e^{-E_i/T}/\mathcal{Z}$ is the Boltzmann weight of eigenstates $|u_i\rangle$ for systems at thermal equilibrium, where $\mathcal{Z} = \sum_i e^{-E_i/T}$. Here, for simplicity, we have set the Boltzmann constant k_B as 1.

In parallel to the Berry phase, for a finite-temperature system undergoing a cyclic adiabatic process, with density matrix denoting as $\rho(t)$ and $t \in [0, 1]$ representing the adiabatic parameter, Uhlmann phase can be defined as the argument of the trace of the density matrix multiplied by an $SU(n)$ unitary transformation W which plays a similar role as the $U(1)$ factor in the Berry phase case, i.e.

$$\Phi_U = \text{ArgTr}[\rho(0)W], \quad (13)$$

as illustrated in Figure 1(b). Here W is the so-called Wilson loop defined as the integration of the Uhlmann connection A_U , i.e.

$$W = \mathcal{P} \exp \left(\int A_U dt \right), \quad (14)$$

where \mathcal{P} denotes the path ordering. The Uhlmann connection A_U is a generalization of Berry connection to an $SU(n)$ gauge connection for mixed states, and is given by

$$A_U = \sum_{m \neq n} \frac{(\sqrt{\lambda_m} - \sqrt{\lambda_n})^2}{\lambda_m + \lambda_n} |u_m\rangle\langle u_m| \frac{d}{dt} |u_n\rangle\langle u_n|. \quad (15)$$

For later convenience, we also define the Uhlmann overlap as

$$\mathcal{F} = \text{Tr}[\rho(0)W]. \quad (16)$$

The Uhlmann has already been used to study several topological systems at finite temperatures [28]. In the rest of this section, we will give a brief derivation of the

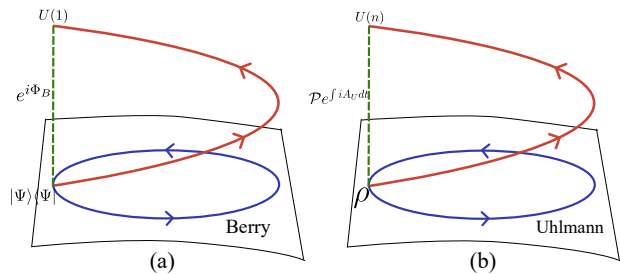


Figure 1. The comparison for the definitions of Berry phase and Uhlmann phase.

Uhlmann connection. And more details can be found in [24].

The concept of Uhlmann connection is based on decomposition of the density matrix as

$$\rho = w w^\dagger, \quad w = \sqrt{\rho} U. \quad (17)$$

Here w can be thought of as the counterpart of the wave function for the mixed states. For a given ρ , the amplitude w contains an arbitrary $U(n)$ phase factor. If we make the replacement $w \rightarrow wU$ where U arbitrary is unitary matrix, ρ will stay the same.

Although the overall phase factor is only a gauge choice, we can determine the relative phase factor U by the following parallel condition proposed by Uhlmann [5]:

$$w_1^\dagger w_2 = w_2^\dagger w_1 = C > 0. \quad (18)$$

Here $C > 0$ means that C is a Hermitian and positive definite matrix. With this condition, the relative phase factor between w_1 and w_2 is uniquely determined as long as the density matrices are always full rank. Consider two different density matrices and their amplitudes $w_1 = \sqrt{\rho_1} U_1$ and $w_2 = \sqrt{\rho_2} U_2$. The parallel condition determines that

$$U_2 U_1^\dagger = \sqrt{\rho_2^{-1}} \sqrt{\rho_1^{-1}} \sqrt{\sqrt{\rho_1} \rho_2 \sqrt{\rho_1}}. \quad (19)$$

The above result is a finite version of the Uhlmann connection. Here ρ is assumed to be a full-rank matrix, since the inverse of ρ has been used.

For the adiabatic path and the associated density matrix $\rho(t)$, we seek a decomposition of the form $\rho(t) = w(t)w^\dagger(t)$ with $w(t) = \sqrt{\rho}W(t)$, such that adjacent amplitudes $w(t)$ and $w(t+dt)$ satisfy the parallel condition in Eq.(18), namely $w^\dagger(t)w(t+dt) = w^\dagger(t+dt)w(t) > 0$. The Uhlmann connection is defined as the differential generator of $W(t)$, expressed as $W(t) = \mathcal{P} e^{\int_0^t A_U(t') dt'}$, where \mathcal{P} denotes path ordering. Taking the derivative of $W(t)$ yields $dW(t)/dt = A_U(t)W(t)$, which can be rearranged as

$$A_U(t) = \frac{dW(t)}{dt} W^\dagger(t). \quad (20)$$

Then by substituting $\rho(t) = \sum_i \lambda_i(t) |u_i(t)\rangle\langle u_i(t)|$ to above expression, and utilizing Eq.(19), which is derived

from the parallel condition Eq.(18), one can obtain the Uhlmann connection Eq.(15). The detailed steps of this derivation are provided in Appendix A for readers interested in the full mathematical process. One can verify that A_U will transform like an ordinary $U(n)$ non-Abelian gauge field under a gauge transformation.

IV. THE UHLMANN PHASE OF BEC

With the definitions of Uhlmann connection and Uhlmann phase in hand, in this section, we will study the Uhlmann phase of BEC at finite temperature.

By adiabatically tuning the parameters in Hamiltonian Eq.(2), denoted as $\hat{H}_{\mathbf{k}}(t)$ with $t \in [0, 1]$ representing the parameter, the corresponding density operator is given by $\rho(t) = \sum_{\mathbf{n}} \lambda_{\mathbf{n}}(t) |\Psi_{\mathbf{n}}(t)\rangle \langle \Psi_{\mathbf{n}}(t)|$ in temperature T . Here, $\lambda_{\mathbf{n}}(t) = e^{-E_{\mathbf{n}}(t)/T} / \mathcal{Z}(t)$ where $\mathcal{Z}(t) = \sum_{\mathbf{n}} e^{-E_{\mathbf{n}}(t)/T}$, and the states $|\Psi_{\mathbf{n}}(t)\rangle$ are defined in Eq.(10). By noting Eq.(11), one can see that the density operator $\rho(t)$ at each t also corresponds to a point $z(t)$ in the Poincare disk, which can be parameterized as

$$z(t) = \tanh \frac{r(t)}{2} e^{i\theta(t)}. \quad (21)$$

This correspondence gives us a geometric way to visualize the Uhlmann process for the BEC, i.e. the density operators $\rho(t)$ with $t \in [0, 1]$ corresponds to a path in the Poincare disk, as shown in Figure 2.

Thus, by substituting the expression Eq.(11) for the states $|\Psi_{\mathbf{n}}\rangle$ into the definition of Uhlmann connection Eq.(15), and making use of the properties of operator $D(\zeta)$ and its Euler decomposition Eq.(9), after some straightforward but tedious calculations (see appendix B for more details), one can obtain the Uhlmann connection of BEC

$$A_U = -i\eta \left[\dot{\theta} \sinh^2 r K_0 + (\dot{r} \sin \theta + \frac{1}{2} \dot{\theta} \sinh(2r) \cos \theta) K_1 + (\dot{r} \cos \theta - \frac{1}{2} \dot{\theta} \sinh(2r) \sin \theta) K_2 \right], \quad (22)$$

where $\eta = 1 - 1/\cosh(\beta\varepsilon_{\mathbf{k}})$, and $r(t)$, $\theta(t)$ representing the path in the Poincare disk as defined in Eq.(21). Then we need to calculate the Uhlmann overlap

$$\begin{aligned} \mathcal{F}(T) &= \text{Tr}[\rho(0)W] \\ &= \sum_{\mathbf{n}} \lambda_{\mathbf{n}}(0) \langle \mathbf{n} | D^\dagger(\zeta_0) W D(\zeta_0) | \mathbf{n} \rangle \\ &\equiv \sum_{\mathbf{n}} \lambda_{\mathbf{n}}(0) \langle \mathbf{n} | U | \mathbf{n} \rangle, \end{aligned} \quad (23)$$

where we have defined $U = D^\dagger(\zeta_0) W D(\zeta_0)$, and $\lambda_{\mathbf{n}}(0) = e^{-E_{\mathbf{n}}(0)/T} / \mathcal{Z}$. We note that the Uhlmann connection Eq.(22) is a linear combination of the $\mathfrak{su}(1, 1)$ generators, thus, the Uhlmann Wilson operator W corresponds to an element in the $SU(1, 1)$ group, which is similar to the time evolution operator of the BEC. Meanwhile, the

operator $D(\zeta_0)$ is also an exponential of a linear combination of the $\mathfrak{su}(1, 1)$ Lie algebra generators, and thus corresponds to an element in the $SU(1, 1)$ group. Consequently, the operator $U = D^\dagger(\zeta_0) W D(\zeta_0)$ is a product of three $SU(1, 1)$ group elements, which itself corresponds to an element in the $SU(1, 1)$ group. Since every element of the $SU(1, 1)$ group has the so-called normal order decomposition and the operator U corresponds to an element in this $SU(1, 1)$ group, thus U has normal order decomposition as [33, 34]

$$U = e^{\mu K^+} e^{\nu K_0} e^{\mu' K^-}, \quad (24)$$

where $K^+ = a_{\mathbf{k}}^\dagger a_{-\mathbf{k}}^\dagger$, $K^- = a_{\mathbf{k}} a_{-\mathbf{k}}$. And the factors μ , μ' and ν can be calculated numerically, which we will discuss soon. Then, by doing Taylor expansion on the exponential terms of Eq.(24), and keeping the non-zero terms, we have

$$\begin{aligned} \langle \mathbf{n} | U | \mathbf{n} \rangle &= \sum_{m=0}^{\min\{n_1, n_2\}} \frac{e^{\frac{\nu}{2}(n+1)} (e^{-\nu} \mu \mu')^m}{(m!)^2} \frac{n_1! n_2!}{(n_1 - m)! (n_2 - m)!} \\ &= e^{\frac{\nu}{2}(n+1)} {}_2F_1(-n_1, -n_2, 1, e^{-\nu} \mu \mu'), \end{aligned} \quad (25)$$

where ${}_2F_1$ is the hypergeometric function and $n = n_1 + n_2$. Hence, we have the expression for the Uhlmann phase

$$\Phi_U = \text{Arg} \sum_{\mathbf{n}} \lambda_{\mathbf{n}}(0) e^{\frac{\nu}{2}(n+1)} {}_2F_1(-n_1, -n_2, 1, e^{-\nu} \mu \mu'). \quad (26)$$

Noting that A_U/i is Hermitian, thus, U is a unitary operator, which indicates $|\langle \mathbf{n} | U | \mathbf{n} \rangle| < 1$. Hence, in above expression, the summation converges and Φ_U can be calculated numerically by choosing suitable cutoffs for n_1, n_2 .

A. Analytical result for circle paths

To compute the Uhlmann phase, the difficult part is the Uhlmann Wilson loop Eq.(14) which is a path ordering product $W = \mathcal{P} \exp \left(\int A_U dt \right)$. Since A_U with different parameters usually do not commute, the path ordering product is quite non-trivial and has to be computed numerically in general.

However, for the circle path whose center coincides with the center of the Poincare disk as shown in Figure 2(a), we can analytically compute W . For this kind of path, r is constant, thus, the \dot{r} terms in Eq.(22) vanish. In this case, we define the Wilson line along an arc as

$$W(\theta) = \mathcal{P} \exp \left(\int_0^\theta A_U(r, \theta') d\theta' \right), \quad (27)$$

where we have converted the integration over the parameter t to one over θ' . It satisfies the following differential

equation

$$\begin{aligned} \frac{dW(\theta)}{d\theta} &= A_U W(\theta), \\ A_U &= -U_1 \left[K_1 \cosh r + K_0 \sinh r \right] U_1^\dagger \cdot (i\eta \sinh r). \end{aligned} \quad (28)$$

Here $U_1 = e^{i\theta K_0}$. If we set $W = U_1 \widetilde{W}$, the above equation is simplified to

$$\begin{aligned} \frac{d\widetilde{W}}{d\theta} &= \left[U_1^\dagger A_U U_1 - U_1^\dagger \frac{dU_1}{d\theta} \right] \widetilde{W} \\ &= \left[-i\eta \sinh r (K_1 \cosh r + K_0 \sinh r) - iK_0 \right] \widetilde{W}. \end{aligned} \quad (29)$$

Now the terms inside the bracket do not depend on θ . It is easy to solve the above equation to find that

$$W(2\pi) = e^{2\pi i K_0} e^{-2\pi i \left[K_0 + \eta \sinh r (K_1 \cosh r + K_0 \sinh r) \right]}. \quad (30)$$

B. General numerical method for calculating Uhlmann phase of BEC

For a general path, it is difficult to calculate the Uhlmann Wilson loop operator analytically. Thus, we resort to the help of the representation theory of $SU(1,1)$ group, i.e. the Uhlmann Wilson loop operator uniquely corresponds to a matrix of the $SU(1,1)$ group.

This correspondence can be seen by noticing that the Uhlmann connection Eq.(22) is a linear combination of the $\mathfrak{su}(1,1)$ Lie algebra. On the other hand, the $\mathfrak{su}(1,1)$ Lie algebra also has a matrix representation, i.e. the operators $K_{0,1,2}$ corresponds to the matrices

$$K_0 \leftrightarrow \sigma_z/2, \quad K_1 \leftrightarrow i\sigma_y/2, \quad K_2 \leftrightarrow -i\sigma_x/2, \quad (31)$$

where $\sigma_{x,y,z}$ are the three Pauli matrices. One can verify that the matrices $\{\sigma_z/2, i\sigma_y/2, -i\sigma_x/2\}$ also satisfy the commutation relation Eq.(4) of $\mathfrak{su}(1,1)$ Lie algebra. By replacing the operators $K_{0,1,2}$ with their corresponding matrices, one can obtain the matrix representation of the Uhlmann connection A_U . Then, one have the corresponding matrix $\mathcal{W} = \mathcal{P}e^{\int A_U dt}$, which belong to the $SU(1,1)$ group, of the Uhlmann Wilson loop operator. We note that the matrix can be calculated numerically by slicing the path into N pieces, i.e.

$$\mathcal{W} = \prod_{i=1}^N e^{A_U(t_i) \Delta t}. \quad (32)$$

Similarly, one can obtain the matrices corresponding to the operators K^\pm , i.e. $K^+ \leftrightarrow \sigma^+$, $K^- \leftrightarrow -\sigma^-$, where $\sigma^\pm = (\sigma_x \pm i\sigma_y)/2$. Thus, one can calculate the corresponding matrix of operator $D(\zeta_0)$ defined in Eq.(8), i.e. $D(\zeta_0) = e^{-\zeta_0 \sigma^+ - \zeta_0^* \sigma^-}$. As a result, the normal order decomposition of Eq.(24) can be cast on the matrix

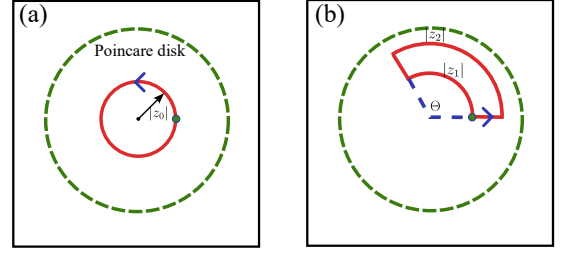


Figure 2. The schematics for the paths of adiabatic Uhlmann process in the Poincare disk, where the red solid lines are the paths, and the green dots are initial points, and the blue arrows indicate the direction of the adiabatic process. (a) Circle path with center coincide with the center of the Poincare disk and radius $|z_0| = \tanh(r_0/2)$. (b) The inner arc has radius $|z_1| = \tanh(r_1/2)$ and the outer arc has radius $|z_2| = \tanh(r_2/2)$.

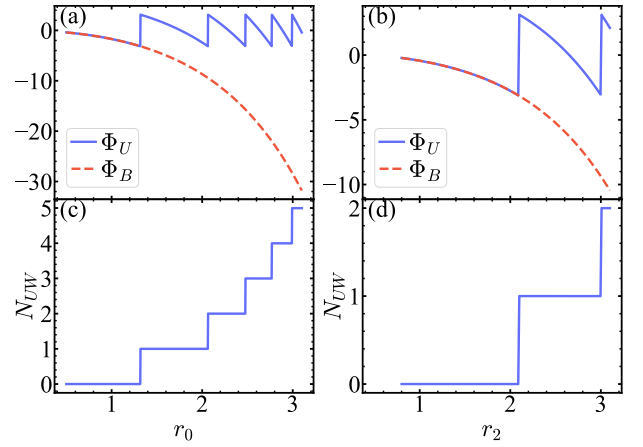


Figure 3. Comparison between the Uhlmann phase in low temperature limit ($T = 0.01$ here) and the Berry phase at zero temperature. (a) The adiabatic path is the one in Figure 2(a) with varying r_0 . (b) The adiabatic path is the one in Figure 2(b) with $r_1 = 1/2$ and varying r_2 . (c) and (d) show the values of N_{UW} for the cases in (a) and (b), respectively.

representation level, which is just the Gaussian decomposition of the matrix $\mathcal{U} = \mathcal{D}^\dagger(\zeta_0) \mathcal{W} \mathcal{D}(\zeta_0)$, i.e. Eq.(24) corresponds to

$$\mathcal{U} = \begin{pmatrix} 1 & \mu \\ 0 & 1 \end{pmatrix} \begin{pmatrix} e^{\frac{\nu}{2}} & 0 \\ 0 & e^{-\frac{\nu}{2}} \end{pmatrix} \begin{pmatrix} 1 & 0 \\ -\mu' & 1 \end{pmatrix}. \quad (33)$$

Hence, one can readily obtain the factors μ, μ' and ν in terms of the matrix elements of \mathcal{U} , which can be calculated numerically in general [33]

$$\mu = \frac{\mathcal{U}_{12}}{\mathcal{U}_{22}}, \quad \mu' = -\frac{\mathcal{U}_{21}}{\mathcal{U}_{22}}, \quad \nu = -2 \ln \mathcal{U}_{22}. \quad (34)$$

Then one can substitute these factors to Eq.(26), and take proper cutoff for the energy level for n_1 and n_2 to calculate the Uhlmann phase.

V. THE UHLMANN PHASE WINDING OF BEC

Having discussed the general method of calculating the Uhlmann phase of BEC, in this section, we will present the numerical results of the Uhlmann phase for different paths on the Poincare disk. These results reveal the unique feature of the Uhlmann phase in the BEC system. Without loss of generality, we assume that the eigenenergy of the quasi-particles is fixed to $\varepsilon_{\mathbf{k}} = 1$ in our numerical calculations. It also serves as an energy unit in the following numerical results.

We first consider the adiabatic process where the path is a circle on the Poincare disk with the center located at the origin of the Poincare disk as shown in Figure 2(a). The parameter equations of this path are

$$r(t) = r_0, \quad \theta(t) = 2\pi t, \quad (35)$$

where r_0 is a constant, and $t \in [0, 1]$. Since the Uhlmann phase is a finite temperature generalization of Berry phase, one may expect that the Uhlmann phase would approach the Berry phase in the zero temperature limit. This is true for previous studies of Uhlmann phase of topological models [28] or spin systems [29]. However, this is not exactly the case for the BEC. The Berry phase of the $SU(1, 1)$ coherent states for the adiabatic process with path described by Eq.(35) is [50]

$$\Phi_B = -2\pi \sinh^2 \frac{r_0}{2}. \quad (36)$$

Note that the above Berry phase takes values in negative real numbers. The comparison between the Uhlmann phase and Berry phase is shown in Figure 3(a). One can see that the Uhlmann phase coincide with Berry phase only when r_0 is small. The reason is that the Uhlmann phase by definition of Eq.(13) is the phase angle of the Uhlmann overlap $\mathcal{F}(T)$, which indicating that $\Phi_U \in [-\pi, \pi)$. Thus, for the BEC case, the Uhlmann phase can be different from the Berry phase by some multiples of 2π . More explicitly, we have

$$\lim_{T \rightarrow 0} \Phi_U = \Phi_B + 2\pi N_{UW}. \quad (37)$$

In Fig. 3(c), we show the values of N_{UW} varying with the radius r_0 of a circle path. However, one may wonder whether the 2π -multiple makes any difference, since the Berry phase is just the phase factor acquired by the ground state in the adiabatic evolution $|G(1)\rangle = e^{i\Phi_B}|G(0)\rangle$. Actually, as we will see later, this 2π -multiple does have its meaning, and can have measurable effect once we consider the behavior of the Uhlmann overlap in the finite temperature range.

In order to provide a better visualization of how the Uhlmann phases change with temperature, in Figure 4(a)-(c), we plot the trajectories of the Uhlmann fidelity $\mathcal{F}(T)$ on the complex plane as the temperature varies from very low as $T/\varepsilon_{\mathbf{k}} = 0.01$ to very high as $T/\varepsilon_{\mathbf{k}} = 500$. The adiabatic paths are still circles on the Poincare disk

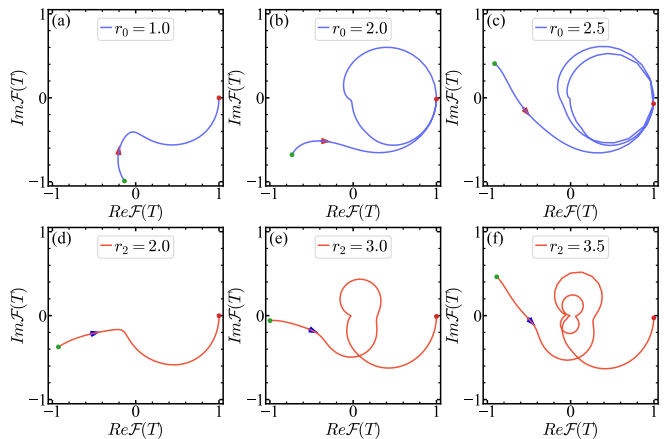


Figure 4. $\mathcal{F}(T)$ from $T/\varepsilon_{\mathbf{k}} = 0.01$ to $T/\varepsilon_{\mathbf{k}} = 500$. The direction of the arrow indicates that the temperature is from low to high. The cutoff of energy level is taken as $n_1 = n_2 = 50$. (a)-(c) The adiabatic path is the one in Figure 2(a). (d)-(f) The adiabatic path is the one in Figure 2(b) with $r_1 = 0.5$.

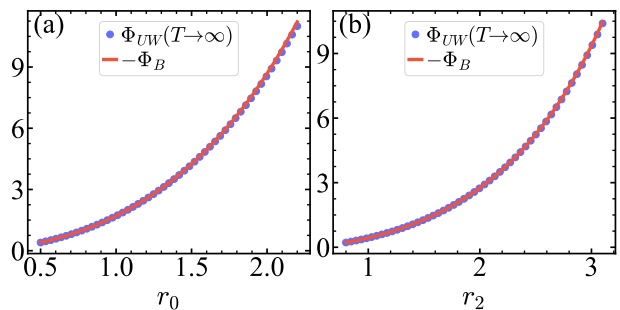


Figure 5. The comparison between the Uhlmann phase winding Φ_{UW} and the negative of Berry phase $-\Phi_B$ for (a) the path shown in Figure 2(a) and (b) the path shown in Figure 2(b).

as in Figure 2 (a). From these figures, we can see that as the circle radius r_0 increases, the Uhlmann overlap starts to circle around the origin of the complex plane as the temperature increases. And as $T \rightarrow \infty$, the Uhlmann phase approach to 0, which is the same as previous studies [28].

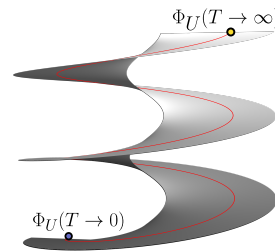


Figure 6. Schematics for the Uhlmann phase takes values in a Riemann surface as the temperature increases from zero temperature limit to infinite temperature limit.

To have a better understanding of the winding behavior of the Uhlmann overlap $\mathcal{F}(T)$, we can study the total degrees that the Uhlmann phase winds around the origin as the temperature increases from zero to infinity. This consideration suggests the following definition of Uhlmann phase winding

$$\Phi_{UW}(T) = \int_0^T \partial_{T'} \Phi_U(T') dT'. \quad (38)$$

In practice, we computed the Uhlmann phase winding numerically by integrating from $T = 0.01$ to $T = 500$. In Figure 5 (a), we plot the Uhlmann phase winding as a function of the path radius r_0 . One can see that the Uhlmann phase winding Φ_{UW} always perfectly agrees with $-\Phi_B$. From this numerical result, one can deduce that

$$\Phi_{UW}(T \rightarrow \infty) = -\Phi_B, \quad (39)$$

In other words, the total degree that the Uhlmann phase winds from zero to infinite temperature is equal to negative of the Berry phase at zero temperature. This result can also be understood as follows. Since Uhlmann phase is always zero at infinite T , we find that

$$\Phi_{UW}(T \rightarrow \infty) = \lim_{T \rightarrow \infty} \Phi_U - \lim_{T \rightarrow 0} \Phi_U + 2\pi N_{UW} = -\Phi_B, \quad (40)$$

where Eq.(37) has been used. Thus, the 2π multiple in the Berry phase is related to the Uhlmann phase winding. And as we propose a method to observe the Uhlmann phase, hence, this 2π multiple in Berry phase can have measurable effect.

One may wonder whether the above result of Eq.(39) is only valid for the circular symmetric paths. To answer this question, we also calculate the Uhlmann phase for adiabatic paths that enclose a sector of the Poincare disk as shown in Figure 2(b), with the inner radius $|z_1| = \tanh(r_1/2)$ and outer radius $|z_2| = \tanh(r_2/2)$. In our numerical calculations, we always fix the arc angle as $\Theta = 2\pi/3$ and the inner radius as $r_1 = 1/2$. Then the Uhlmann phase in the zero temperature limit is plotted as a function of outer radius r_2 in comparison the Berry phase in Figure 3(b). Again, one can see that they are different by some multiple of 2π .

In Figure 4(d)-(f), the curves of the Uhlmann overlap $\mathcal{F}(T)$ on the complex plane display very similar behaviors as before. Therefore, we can still compute the Uhlmann phase winding for this type of paths and the resulting Φ_{UW} also agrees with $-\Phi_B$ as shown in Figure 5(b). These results of sector-like paths suggest that the relation of Eq.(39) between the Uhlmann phase winding and Berry phase is not limited to the circular paths but a general feature of the BEC.

Thus, we conclude that the Uhlmann phase, as a function of temperature, winds from $\Phi(T \rightarrow 0)$ to 0 as the temperature increases from the zero-temperature limit to the infinite-temperature limit. To further reveal the geometric meaning of the Uhlmann phase winding, it is

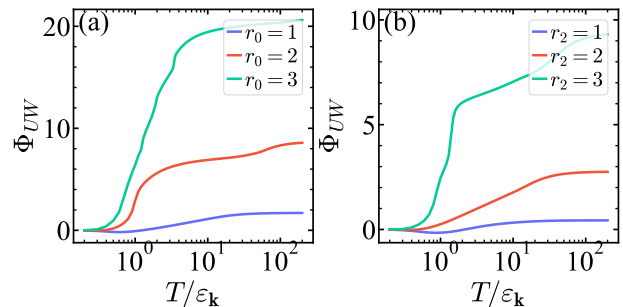


Figure 7. The Uhlmann phase winding $\Phi_{UW}(T)$ varying as the temperature T increases for (a) the path shown in Figure 2(a) and (b) for the path shown in Figure 2(b). Note that the x-axis is in logarithmic scale.

suggested that the Uhlmann phase takes values in a Riemann surface. Actually, we can view the Uhlmann phase as a multiple valued function $\ln(\mathcal{F}/|\mathcal{F}|)/i$. It can be converted into a single valued function which is defined on a Riemann surface of $\ln(z)$ as shown in Figure 6. Then the geometric meaning of N_{UW} is just the number of times that the Uhlmann phase circles around the branch point on the Riemann surface.

On the other hand, one may wonder whether it is meaningful to consider the Uhlmann phase as $T \rightarrow \infty$, since the BEC collapses when the temperature is above the transition temperature T_c , and the Bogoliubov approximation becomes invalid. To address this concern, we show the Uhlmann phase winding $\Phi_{UW}(T)$ with varying T in Figure 7 for the two kinds of paths in Figure 2 respectively. These results suggest that the Uhlmann phase winding $\Phi_{UW}(T)$ mostly increases in low temperature. Our numerical results indicate that when the temperature rises to approximately $20\varepsilon_k$, the Uhlmann phase winding $\Phi_{UW}(T)$ reaches about 90% of its total value $\Phi_{UW}(T \rightarrow \infty)$. Consequently, we anticipate that the Uhlmann winding occurs when the quasiparticle energy ε_k is much lower than the critical temperature T_c . This condition can be met by choosing an appropriate momentum.

The Uhlmann phase is applicable not only to finite-temperature systems but also to mixed states in open quantum systems. And the density matrix at infinite temperature can also describe the maximally mixed states in open quantum system. While it is known that maximally mixed states always have zero Uhlmann phase, the converse is not necessarily true; a density matrix that differs from the identity matrix can also yield a vanishing Uhlmann phase. This observation raises interesting questions for future research, such as whether Uhlmann phase winding occurs in open quantum systems, and if a Uhlmann phase winding number can be meaningfully extracted and interpreted for such systems.

VI. PROPOSAL FOR EXPERIMENTAL MEASUREMENT OF UHLMANN PHASE OF BEC

The experimental implementations to measure Uhlmann phase have been proposed for various systems, such as the photonic systems [8], and spin systems [29]. Recently, in [51], the Uhlmann phase has been measured in topological system by using an IBM's quantum computing platform. In these cases, the experimental schemes to measure Uhlmann phase are similar, i.e. based on a purification and interference scheme. Firstly, one needs to find a purification $|w(0)\rangle$ of the density matrix ρ_0 . Here, $|w(0)\rangle$ is a state in the Fock space $\mathbb{F}_S \otimes \mathbb{F}_A$, where \mathbb{F}_S is the Fock space of the physical system S and \mathbb{F}_A denotes the Fock space of the ancilla system A . Here, the ancilla system is another BEC. By doing partial trace over the ancilla system, one obtains the original density matrix $\rho_0 = \text{Tr}_A |w(0)\rangle\langle w(0)|$. Secondly, one needs to find a time evolution process for the purified state $|w(t)\rangle = U(t)|w(0)\rangle$, such that $\text{Arg}\langle w(0)|w(1)\rangle = \text{Arg}(\rho_0 \mathcal{P}e^{\int A_V dt}) = \Phi_U$. Finally, one can use an interferometer device, in the BEC case the atomic interferometer, to measure the Uhlmann phase Φ_U [47]. A similar interference measurement method has been used in the so-called $SU(1,1)$ interferometer [52–54].

We start from finding the purification of the density matrix $\rho(t) = \sum_{\mathbf{n}} \lambda_{\mathbf{n}} |\Psi_{\mathbf{n}}(t)\rangle\langle \Psi_{\mathbf{n}}(t)|$ at parameter t . The ancilla system we choose here is another BEC. A simple purified state is $|w_0(t)\rangle = \sum_{\mathbf{n}} \sqrt{\lambda_{\mathbf{n}}} |\Psi_{\mathbf{n}}(t)\rangle \otimes |\tilde{\Psi}_{\mathbf{n}}(t)\rangle$, where $|\tilde{\Psi}_{\mathbf{n}}\rangle$'s are exactly the same quasi-particles state as $|\Psi_{\mathbf{n}}\rangle$ but live in the Fock space \mathbb{F}_A of the ancilla system. However, such a purification is not unique, any unitary transformation of the ancilla system

$$|w(t)\rangle = \sum_{\mathbf{n}} \sqrt{\lambda_{\mathbf{n}}} |\Psi_{\mathbf{n}}(t)\rangle \otimes \tilde{U}_g(t) |\tilde{\Psi}_{\mathbf{n}}(t)\rangle \quad (41)$$

can give another purification of the density matrix. This gives us a gauge redundancy. In order to make $\text{Arg}\langle w(0)|w(1)\rangle$ gives us the correct Uhlmann phase, we need to properly choose the gauge. Such a gauge can be identified by imposing the so-called parallel transport condition, i.e. [24]

$$\text{Im}\langle w(t) | \frac{d}{dt} |w(t)\rangle = 0. \quad (42)$$

Actually, this condition can be satisfied by choose the gauge as $\tilde{U}_g(t)(t) = \mathcal{P}e^{\int_0^t A_V(t') dt'}$ [24].

On the other hand, the quasi-particle state $|\Psi_{\mathbf{n}}(t)\rangle$ can also be obtained by time evolution of $|\Psi_{\mathbf{n}}(0)\rangle$ under a suitable chosen Hamiltonian, i.e. $|\Psi_{\mathbf{n}}(t)\rangle = U_d(t) |\Psi_{\mathbf{n}}(0)\rangle$. Hence, we have

$$|w(t)\rangle = \sum_{\mathbf{n}} \sqrt{\lambda_{\mathbf{n}}} U_d(t) |\Psi_{\mathbf{n}}(0)\rangle \otimes [\tilde{U}_g(t) \tilde{U}_d(t)] |\tilde{\Psi}_{\mathbf{n}}(0)\rangle \quad (43)$$

Then by using Eq.(11), we can rewrite the above equation as

$$\begin{aligned} |w(t)\rangle &= \sum_{\mathbf{n}} \sqrt{\lambda_{\mathbf{n}}} U_d(t) D(\zeta_0) |\mathbf{n}\rangle_S \otimes \tilde{U}_g(t) \tilde{U}_d(t) \tilde{D}(\zeta_0) |\mathbf{n}\rangle_A \\ &\equiv U_d(t) D(\zeta_0) \tilde{U}_g(t) \tilde{U}_d(t) \tilde{D}(\zeta_0) |m\rangle, \end{aligned} \quad (44)$$

where we have defined $|m\rangle = \sum_{\mathbf{n}} \sqrt{\lambda_{\mathbf{n}}} |\mathbf{n}\rangle_S \otimes |\mathbf{n}\rangle_A$. Actually, the state $|m\rangle$ is nothing but the coherent state of a two-component BEC, if we view the bosonic modes in the physical system and the ones in the ancilla system as two species of bosons in the two-component BEC. More specifically, we can define the vacuum of the composite system as $|0\rangle = |0\rangle_S \otimes |0\rangle_A$. Then the state $|m\rangle$ can be written as

$$\begin{aligned} |m\rangle &= \sum_{\mathbf{n}} \sqrt{\lambda_{\mathbf{n}}} \frac{a_{\mathbf{k}}^{\dagger n_1} a_{-\mathbf{k}}^{\dagger n_2}}{\sqrt{n_1! n_2!}} \frac{\tilde{a}_{\mathbf{k}}^{\dagger n_1} \tilde{a}_{-\mathbf{k}}^{\dagger n_2}}{\sqrt{n_1! n_2!}} |0\rangle \\ &= \frac{1}{\sqrt{\mathcal{Z}}} \sum_{\mathbf{n}} \frac{(e^{-\frac{\varepsilon_{\mathbf{k}}}{2T}} a_{\mathbf{k}}^{\dagger} \tilde{a}_{\mathbf{k}}^{\dagger})^{n_1}}{n_1!} \frac{(e^{-\frac{\varepsilon_{-\mathbf{k}}}{2T}} a_{-\mathbf{k}}^{\dagger} \tilde{a}_{-\mathbf{k}}^{\dagger})^{n_2}}{n_2!} |0\rangle \\ &= \frac{1}{\sqrt{\mathcal{Z}}} \exp(e^{-\frac{\varepsilon_{\mathbf{k}}}{2T}} a_{\mathbf{k}}^{\dagger} \tilde{a}_{\mathbf{k}}^{\dagger} + e^{-\frac{\varepsilon_{-\mathbf{k}}}{2T}} a_{-\mathbf{k}}^{\dagger} \tilde{a}_{-\mathbf{k}}^{\dagger}) |0\rangle, \end{aligned} \quad (45)$$

which is a coherent state of two-component BEC. Here, we have used $\lambda_{\mathbf{n}} = e^{-(n_1+n_2)\varepsilon_{\mathbf{k}}/T} / \mathcal{Z}$. Using similar technique as in Eq.(8), we can rewrite $|m\rangle$ as time evolution of the vacuum state under Hamiltonian H_m

$$|m\rangle = e^{-iH_m} |0\rangle, \quad (46)$$

where $H_m = i\zeta_m (a_{\mathbf{k}}^{\dagger} \tilde{a}_{\mathbf{k}}^{\dagger} + a_{-\mathbf{k}}^{\dagger} \tilde{a}_{-\mathbf{k}}^{\dagger}) + h.c.$, with $\zeta_m = \arctan(e^{-\varepsilon_{\mathbf{k}}/2T})$.

Thus, one can prepare the initial state $|w(0)\rangle$ as follows: starting from the fully condensed state of two-component BEC, i.e. all particles condensed in zero momentum states, and quench the system under the Hamiltonian H_m to get $|m\rangle$, then change quenched Hamiltonian to $H_{\zeta_0} = \zeta_0 (a_{\mathbf{k}}^{\dagger} a_{-\mathbf{k}}^{\dagger} + \tilde{a}_{\mathbf{k}}^{\dagger} \tilde{a}_{-\mathbf{k}}^{\dagger}) + h.c.$, since it can be verified that $e^{-iH_{\zeta_0}} = D(\zeta_0) \tilde{D}(\zeta_0)$, i.e.

$$|w(0)\rangle = e^{-iH_{\zeta_0}} |m\rangle. \quad (47)$$

After this two quench processes, one can obtain the $|w(0)\rangle$ state.

In order to measure the Uhlmann phase in an atomic interferometer, one needs to coherently split the system to two copies (similar to the two arms of Mach-Zehnder interferometer). In Fig. 8, we show the schematics for the interferometric process. Then, making one copy evolve under the time evolution operator $U = U_d(1) \tilde{U}_g(1) \tilde{U}_d(1)$ to obtain $|w(1)\rangle$, i.e.

$$|w(1)\rangle = U |w(0)\rangle \equiv U_d(1) \tilde{U}_g(1) \tilde{U}_d(1) |w(0)\rangle. \quad (48)$$

For the other copy, one needs to imprint a phase factor $e^{i\chi}$ on it by using laser beam [55]. The phase imprinting technique has been experimentally implemented in BEC

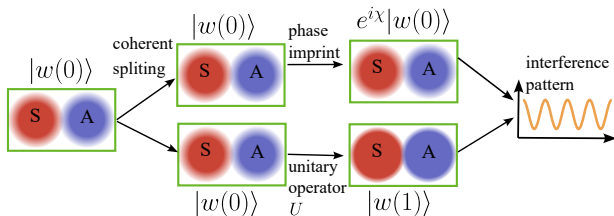


Figure 8. Schematics for the interferometric measurement process. After preparing $|w(0)\rangle$ state, we coherently split the whole system into two copies. One copy is imprinted a phase $e^{i\chi}$ by applying laser beam. The other copy is evolved to $|w(1)\rangle$ state. Then these two copies are brought together to interfere.

system. [56, 57] Finally, one combine the two arms of the atomic interferometer and measure the interference pattern

$$\begin{aligned} & \left| \frac{1}{\sqrt{2}} (e^{i\chi}|w(0)\rangle + |w(1)\rangle) \right|^2 \\ & = 1 + |\langle w(0)|w(1)\rangle| \cos(\chi + \Phi_U). \end{aligned} \quad (49)$$

Thus, by varying χ and repeating this interferometric measurement process, one can obtain the Uhlmann phase from the interference pattern.

VII. CONCLUSION

In this paper, we have investigated the Uhlmann phase for Bose-Einstein condensates at finite temperature. By exploiting the $SU(1,1)$ symmetry of the Bogoliubov Hamiltonian, we derived a general formula for the Uhlmann phase of BECs. Our numerical calculations revealed that, contrary to previous studies, the

Uhlmann phase can differ from the Berry phase in the zero-temperature limit. Furthermore, we uncovered a unique winding behavior of the Uhlmann phase as the temperature increases, where the total winding degree is equal to the negative of the Berry phase at zero temperature. This winding indicates that the Uhlmann phase takes values on a Riemann surface, highlighting its geometric nature.

Our work not only provides a theoretical framework for understanding topological properties of BECs at finite temperature but also proposes an experimental scheme to measure the Uhlmann phase using an atomic interferometer. These results reveal new aspects of the Uhlmann phase and its relationship with the Berry phase in quantum systems at finite temperature, suggesting that the Uhlmann phase can serve as a useful tool to probe topological properties of BECs and other quantum systems.

Future research directions include extending our analysis to two-component or spinor BECs and exploring the effects of interactions and symmetry breaking on the Uhlmann phase. Additionally, studying the Uhlmann phase of BECs in the presence of noise, decoherence, and measurement errors can provide insights into its robustness and sensitivity to these factors.

We anticipate that our work will stimulate further interest and research on the Uhlmann phase and its applications in quantum physics, particularly in the context of topological properties and experimental investigations of mixed-state quantum systems.

ACKNOWLEDGMENTS

CYW is supported by the Shuimu Tsinghua scholar program at Tsinghua University. YH is supported by the National Natural Science Foundation of China under Grant No. 11874272.

Appendix A: Detailed derivation for the expression of the Uhlmann connection Eq.(15)

In this appendix, we provide a detailed derivation of the Uhlmann connection Eq.(15), following the approach in Ref.[24].

For an adiabatic path with associated density matrix $\rho(t)$, we seek a decomposition of the form $\rho(t) = w(t)w^\dagger(t)$ with $w(t) = \sqrt{\rho}W(t)$, such that adjacent amplitudes $w(t)$ and $w(t+dt)$ satisfy the parallel condition in Eq.(18):

$$w^\dagger(t)w(t+dt) = w^\dagger(t+dt)w(t) > 0. \quad (A1)$$

According to Eq.(19), to satisfy the parallel condition, the amplitude should fulfill:

$$W(t+dt)W^\dagger(t) = \sqrt{\rho_2^{-1}}\sqrt{\rho_1^{-1}}\sqrt{\sqrt{\rho_1}\rho_2\sqrt{\rho_1}}, \quad (A2)$$

where $\rho_1 = \rho(t)$ and $\rho_2 = \rho(t+dt)$. By introducing infinitesimal changes $W(t+dt) = W(t) + dW \equiv W(t) + \dot{W}(t)dt$ and $\rho(t+dt) = \rho(t) + d\rho \equiv \rho(t) + \dot{\rho}(t)dt$, where $\dot{W}(t) = dW/dt$ and $\dot{\rho}(t) = d\rho/dt$, Eq.(A1) can then be rewritten as:

$$(W + dW)W^\dagger = (\sqrt{\rho} + d\sqrt{\rho})^{-1}\sqrt{\rho^{-1}}\sqrt{\sqrt{\rho}(\rho + d\rho)\sqrt{\rho}}, \quad (A3)$$

where we've used $\sqrt{\rho + d\rho} = \sqrt{\rho} + d\sqrt{\rho}$. We introduce an auxiliary real parameter s to each differential in the above expression:

$$(W + sdW)W^\dagger = (\sqrt{\rho} + sd\sqrt{\rho})^{-1} \sqrt{\rho^{-1}} \sqrt{\sqrt{\rho}(\rho + sd\rho)\sqrt{\rho}}. \quad (\text{A4})$$

Expanding this expression around $s = 0$ and keeping only first-order terms in s , we obtain the Uhlmann connection:

$$Adt = dWW^\dagger = \left[\frac{d}{ds} (\sqrt{\rho} + sd\sqrt{\rho})^{-1} \right] \Big|_{s=0} \sqrt{\rho} + \rho^{-1} \left[\frac{d}{ds} \sqrt{\sqrt{\rho}(\rho + sd\rho)\sqrt{\rho}} \right] \Big|_{s=0}. \quad (\text{A5})$$

For the first term on the right-hand side, to the leading order in s :

$$(\sqrt{\rho} + sd\sqrt{\rho})^{-1} = \left[\sqrt{\rho}(1 + s\sqrt{\rho^{-1}}d\sqrt{\rho}) \right]^{-1} = (1 - s\sqrt{\rho^{-1}}d\sqrt{\rho})\sqrt{\rho^{-1}}. \quad (\text{A6})$$

Thus,

$$\left[\frac{d}{ds} (\sqrt{\rho} + sd\sqrt{\rho})^{-1} \right] \Big|_{s=0} \sqrt{\rho} = -\sqrt{\rho^{-1}}d\sqrt{\rho}. \quad (\text{A7})$$

In the eigenbasis of ρ , it becomes

$$-\langle u_m | \sqrt{\rho^{-1}}d\sqrt{\rho} | u_n \rangle = -\frac{1}{\sqrt{\lambda_m}} \langle u_m | d\sqrt{\rho} | u_n \rangle. \quad (\text{A8})$$

We define $K(s) = \sqrt{\sqrt{\rho}(\rho + sd\rho)\sqrt{\rho}}$. Then, the second term in Eq.(A5) becomes $\rho^{-1}K'(0)$, where $K'(s) = dK(s)/ds$. Taking the derivative of $[K(s)]^2$ with respect to s :

$$K'(s)K(s) + K(s)K'(s) = \sqrt{\rho}d\rho\sqrt{\rho}. \quad (\text{A9})$$

At $s = 0$, noting that $K(0) = \rho$:

$$K'(0)\rho + \rho K'(0) = \sqrt{\rho}d\rho\sqrt{\rho}. \quad (\text{A10})$$

Taking matrix elements in the eigenbasis of ρ :

$$(\lambda_m + \lambda_n) \langle u_m | K'(0) | u_n \rangle = \sqrt{\lambda_m \lambda_n} \langle u_m | d\rho | u_n \rangle. \quad (\text{A11})$$

Thus, $\rho^{-1}K'(0)$ becomes:

$$\langle u_m | \rho^{-1}K'(0) | u_n \rangle = \frac{\sqrt{\lambda_n}}{\sqrt{\lambda_m}(\lambda_m + \lambda_n)} \langle u_m | d\rho | u_n \rangle. \quad (\text{A12})$$

Noting that $d\rho = d(\sqrt{\rho}\sqrt{\rho}) = d\sqrt{\rho}\sqrt{\rho} + \sqrt{\rho}d\sqrt{\rho}$:

$$\langle u_m | \rho^{-1}K'(0) | u_n \rangle = \frac{\sqrt{\lambda_n}(\sqrt{\lambda_m} + \sqrt{\lambda_n})}{\sqrt{\lambda_m}(\lambda_m + \lambda_n)} \langle u_m | d\sqrt{\rho} | u_n \rangle. \quad (\text{A13})$$

Combining these results, the Uhlmann connection becomes:

$$\langle u_m | Adt | u_n \rangle = \left[-\frac{1}{\sqrt{\lambda_m}} + \frac{\sqrt{\lambda_n}(\sqrt{\lambda_m} + \sqrt{\lambda_n})}{\sqrt{\lambda_m}(\lambda_m + \lambda_n)} \right] \langle u_m | d\sqrt{\rho} | u_n \rangle = \frac{\sqrt{\lambda_n} - \sqrt{\lambda_m}}{\lambda_m + \lambda_n} \langle u_m | d\sqrt{\rho} | u_n \rangle. \quad (\text{A14})$$

Substituting $\sqrt{\rho} = \sum_i \sqrt{\lambda_i} | u_i \rangle \langle u_i |$ to above expression

$$\langle u_m | Adt | u_n \rangle = \frac{\sqrt{\lambda_n} - \sqrt{\lambda_m}}{\lambda_m + \lambda_n} \left[d\sqrt{\lambda_m} \delta_{mn} + \sqrt{\lambda_n} \langle u_m | d | u_n \rangle + \sqrt{\lambda_m} (d \langle u_m |) | u_n \rangle \right], \quad (\text{A15})$$

where δ_{mn} is the Kronecker delta. Since $d(\langle u_m | u_n \rangle) = 0$, we have $(d \langle u_m |) | u_n \rangle = -\langle u_m | d | u_n \rangle$.

Therefore, the final expression for the Uhlmann connection is:

$$\langle u_m | A | u_n \rangle = \frac{(\sqrt{\lambda_n} - \sqrt{\lambda_m})^2}{\lambda_m + \lambda_n} \langle u_m | \frac{d}{dt} | u_n \rangle. \quad (\text{A16})$$

Appendix B: Calculation of the Uhlmann connection for BEC

In this appendix, we will present the detailed derivation of the Uhlmann connection of $SU(1,1)$ coherent states Eq.(22). In order to obtain the Uhlmann connection Eq.(15), we first need to calculate $\langle \Psi_{\mathbf{n}} | \frac{d}{dt} | \Psi_{\mathbf{m}} \rangle$. By using the expression Eq.(11) for $|\Psi_{\mathbf{n}}\rangle$ and noticing the Euler decomposition Eq.(9), we have

$$\begin{aligned} \langle \Psi_{\mathbf{n}} | \frac{d}{dt} | \Psi_{\mathbf{m}} \rangle &= \langle \mathbf{n} | D^\dagger(\zeta) \frac{d}{dt} D(\zeta) | \mathbf{m} \rangle \\ &= i e^{i \frac{n-m}{2} \theta} \langle \mathbf{n} | \left(\dot{\theta} e^{irK_2} K_0 e^{-irK_2} - \dot{r} K_2 - n \dot{\theta} \right) | \mathbf{m} \rangle \\ &= i e^{i \frac{n-m}{2} \theta} \langle \mathbf{n} | \left(\dot{\theta} \cosh rK_0 - \sinh rK_1 - \dot{r} K_2 - n \dot{\theta} \right) | \mathbf{m} \rangle, \end{aligned} \quad (\text{B1})$$

Here $n = n_1 + n_2$ and $m = m_1 + m_2$. In the last step we have used

$$e^{irK_2} K_0 e^{-irK_2} = \cosh rK_0 - \sinh rK_1. \quad (\text{B2})$$

Then substituting above expression to Eq.(15), and noticing the summation is over $\mathbf{m} \neq \mathbf{n}$, we find that

$$A_U = i \sum_{\mathbf{n} \neq \mathbf{m}} f_{\mathbf{n}, \mathbf{m}} e^{i\theta K_0} e^{-irK_2} | \mathbf{n} \rangle \langle \mathbf{n} | \left(-\dot{\theta} \sinh rK_1 - \dot{r} K_2 \right) | \mathbf{m} \rangle \langle \mathbf{m} | e^{irK_2} e^{-i\theta K_0}. \quad (\text{B3})$$

Here we defined $f_{\mathbf{n}, \mathbf{m}} = \frac{(\sqrt{\lambda_{\mathbf{n}}} - \sqrt{\lambda_{\mathbf{m}}})^2}{\lambda_{\mathbf{n}} + \lambda_{\mathbf{m}}}$. Noticing that $K_1 = (K^+ + K^-)/2$, $K_2 = (K^+ - K^-)/2i$, thus, only terms with $\mathbf{m} = \mathbf{n} \pm (1, 1)$ contribute non-zero values, other terms vanish.

Also, when $\mathbf{m} = \mathbf{n} \pm (1, 1)$, we have $f_{\mathbf{n}, \mathbf{m}} = 1 - 1/\cosh(\beta\varepsilon_{\mathbf{k}}) \equiv \eta$ which is a constant and can be pulled out the summations. Therefore, we can make use of the completeness relation to simplify A_U as follows

$$\begin{aligned} A_U &= -i\eta \sum_{\mathbf{n}} e^{i\theta K_0} e^{-irK_2} (\dot{\theta} \sinh rK_1 + \dot{r} K_2) | \mathbf{n} \rangle \langle \mathbf{n} | e^{irK_2} e^{-i\theta K_0} \\ &= -i\eta e^{i\theta K_0} e^{-irK_2} (\dot{\theta} \sinh rK_1 + \dot{r} K_2) e^{irK_2} e^{-i\theta K_0}, \end{aligned} \quad (\text{B4})$$

Then by using the transformation relations [34]

$$e^{i\theta K_0} K_2 e^{-i\theta K_0} = \sin \theta K_1 + \cos \theta K_2, \quad (\text{B5})$$

$$e^{-irK_2} K_1 e^{irK_2} = \sinh rK_0 + \cosh rK_1, \quad (\text{B6})$$

$$e^{i\theta K_0} K_1 e^{-i\theta K_0} = \cos \theta K_1 - \sin \theta K_2, \quad (\text{B7})$$

we can obtain Eq.(22).

- | | |
|---|---|
| <p>[1] M. V. Berry, Quantal phase factors accompanying adiabatic changes, <i>Proceedings of the Royal Society of London. A. Mathematical and Physical Sciences</i> 392, 45 (1984).</p> <p>[2] J. Zak, Berry's phase for energy bands in solids, <i>Phys. Rev. Lett.</i> 62, 2747 (1989).</p> <p>[3] D. J. Thouless, M. Kohmoto, M. P. Nightingale, and M. den Nijs, Quantized Hall Conductance in a Two-Dimensional Periodic Potential, <i>Phys. Rev. Lett.</i> 49, 405 (1982).</p> <p>[4] B. Mera, C. Vlachou, N. Paunković, and V. R. Vieira, Uhlmann Connection in Fermionic Systems Undergoing Phase Transitions, <i>Phys. Rev. Lett.</i> 119, 015702 (2017).</p> <p>[5] A. Uhlmann, Parallel transport and "quantum holonomy" along density operators, <i>Reports on Mathematical Physics</i> 24, 229 (1986).</p> | <p>[6] A. Uhlmann, A gauge field governing parallel transport along mixed states, <i>Lett Math Phys</i> 21, 229 (1991).</p> <p>[7] A. Uhlmann, Density operators as an arena for differential geometry, <i>Reports on Mathematical Physics</i> 33, 253 (1993).</p> <p>[8] M. Ericsson, A. K. Pati, E. Sjöqvist, J. Brännlund, and D. K. L. Oi, Mixed State Geometric Phases, Entangled Systems, and Local Unitary Transformations, <i>Phys. Rev. Lett.</i> 91, 090405 (2003).</p> <p>[9] M. Ericsson, E. Sjöqvist, J. Brännlund, D. K. L. Oi, and A. K. Pati, Generalization of the geometric phase to completely positive maps, <i>Phys. Rev. A</i> 67, 020101 (2003).</p> <p>[10] A. D. Kiselev and V. V. Kesaev, Interferometric and Uhlmann phases of mixed polarization states, <i>Phys. Rev. A</i> 98, 033816 (2018).</p> <p>[11] K. Singh, D. M. Tong, K. Basu, J. L. Chen, and J. F.</p> |
|---|---|

- Du, Geometric phases for nondegenerate and degenerate mixed states, *Phys. Rev. A* **67**, 032106 (2003).
- [12] J. Tidström and E. Sjöqvist, Uhlmann’s geometric phase in presence of isotropic decoherence, *Phys. Rev. A* **67**, 032110 (2003).
- [13] D. M. Tong, E. Sjöqvist, L. C. Kwek, and C. H. Oh, Kinematic Approach to the Mixed State Geometric Phase in Nonunitary Evolution, *Phys. Rev. Lett.* **93**, 080405 (2004).
- [14] X. Wang, X.-Y. Hou, Z. Zhou, H. Guo, and C.-C. Chien, Uhlmann phase of coherent states and the Uhlmann-Berry correspondence, *SciPost Physics Core* **6**, 024 (2023).
- [15] A. Carollo, B. Spagnolo, and D. Valenti, Uhlmann curvature in dissipative phase transitions, *Sci Rep* **8**, 9852 (2018).
- [16] Z. Gao and Y. He, Quantum quench dynamics of Berry and Uhlmann phases in topological systems, *Phys. Rev. B* **108**, 085126 (2023).
- [17] H. Guo, X.-Y. Hou, Y. He, and C.-C. Chien, Dynamic process and Uhlmann process: Incompatibility and dynamic phase of mixed quantum states, *Phys. Rev. B* **101**, 104310 (2020).
- [18] Y. He, H. Guo, and C.-C. Chien, Thermal Uhlmann-Chern number from the Uhlmann connection for extracting topological properties of mixed states, *Phys. Rev. B* **97**, 235141 (2018).
- [19] Y. He and C.-C. Chien, Uhlmann holonomy against Lindblad dynamics of topological systems at finite temperatures, *Phys. Rev. B* **106**, 024310 (2022).
- [20] X.-Y. Hou, Q.-C. Gao, H. Guo, Y. He, T. Liu, and C.-C. Chien, Ubiquity of zeros of the Loschmidt amplitude for mixed states in different physical processes and its implication, *Phys. Rev. B* **102**, 104305 (2020).
- [21] B. Mera, C. Vlachou, N. Paunković, V. R. Vieira, and O. Viyuela, Dynamical phase transitions at finite temperature from fidelity and interferometric Loschmidt echo induced metrics, *Phys. Rev. B* **97**, 094110 (2018).
- [22] A. Pi, Y. Zhang, Y. He, and C.-C. Chien, Proxy ensemble geometric phase and proxy index of time-reversal invariant topological insulators at finite temperatures, *Phys. Rev. B* **105**, 085418 (2022).
- [23] J. Villavicencio, E. Cota, F. Rojas, J. A. Maytorena, and D. M. Galindo, Uhlmann phase in composite systems with entanglement, *Phys. Rev. A* **104**, 042204 (2021).
- [24] O. Viyuela, A. Rivas, and M. A. Martin-Delgado, Symmetry-protected topological phases at finite temperature, *2D Mater.* **2**, 034006 (2015).
- [25] Y. Zhang, A. Pi, Y. He, and C.-C. Chien, Comparison of finite-temperature topological indicators based on Uhlmann connection, *Phys. Rev. B* **104**, 165417 (2021).
- [26] Z. Huang and D. P. Arovas, Topological Indices for Open and Thermal Systems Via Uhlmann’s Phase, *Phys. Rev. Lett.* **113**, 076407 (2014).
- [27] O. Viyuela, A. Rivas, and M. A. Martin-Delgado, Uhlmann Phase as a Topological Measure for One-Dimensional Fermion Systems, *Phys. Rev. Lett.* **112**, 130401 (2014).
- [28] O. Viyuela, A. Rivas, and M. A. Martin-Delgado, Two-Dimensional Density-Matrix Topological Fermionic Phases: Topological Uhlmann Numbers, *Phys. Rev. Lett.* **113**, 076408 (2014).
- [29] X.-Y. Hou, H. Guo, and C.-C. Chien, Finite-temperature topological phase transitions of spin- j systems in Uhlmann processes: General formalism and experimental protocols, *Phys. Rev. A* **104**, 023303 (2021).
- [30] D. Morachis Galindo, F. Rojas, and J. A. Maytorena, Topological Uhlmann phase transitions for a spin- j particle in a magnetic field, *Phys. Rev. A* **103**, 042221 (2021).
- [31] J. Villavicencio, E. Cota, F. Rojas, J. A. Maytorena, D. Morachis Galindo, and F. Nieto-Guadarrama, Thermal Uhlmann phase in a locally driven two-spin system, *Phys. Rev. A* **107**, 062222 (2023).
- [32] C. Chin, R. Grimm, P. Julienne, and E. Tiesinga, Feshbach resonances in ultracold gases, *Rev. Mod. Phys.* **82**, 1225 (2010).
- [33] A. Perelomov, *Generalized Coherent States and Their Applications* (Springer-Verlag, Berlin Heidelberg, 1986).
- [34] R. R. Puri, *Mathematical Methods of Quantum Optics* (Springer-Verlag, Berlin Heidelberg, 2001).
- [35] C. M. Caves and B. L. Schumaker, New formalism for two-photon quantum optics. I. Quadrature phases and squeezed states, *Phys. Rev. A* **31**, 3068 (1985).
- [36] Y.-Y. Chen, P. Zhang, W. Zheng, Z. Wu, and H. Zhai, Many-body echo, *Phys. Rev. A* **102**, 011301 (2020).
- [37] Y. Cheng and Z.-Y. Shi, Many-body dynamics with time-dependent interaction, *Phys. Rev. A* **104**, 023307 (2021).
- [38] C. Lv, R. Zhang, and Q. Zhou, $SU(1,1)$ echoes for Breathers in Quantum Gases, *Phys. Rev. Lett.* **125**, 253002 (2020).
- [39] C. Lyu, C. Lv, and Q. Zhou, Geometrizing Quantum Dynamics of a Bose-Einstein Condensate, *Phys. Rev. Lett.* **125**, 253401 (2020).
- [40] J. Zhang, X. Yang, C. Lv, S. Ma, and R. Zhang, Quantum dynamics of cold atomic gas with $SU(1,1)$ symmetry, *Phys. Rev. A* **106**, 013314 (2022).
- [41] P. Zhang and Y. Gu, Periodically and quasi-periodically driven dynamics of Bose-Einstein condensates, *SciPost Physics* **9**, 079 (2020).
- [42] C.-Y. Wang and Y. He, The quantum dynamics of two-component Bose-Einstein condensate: An $Sp(4, R)$ symmetry approach, *J. Phys.: Condens. Matter* **34**, 455401 (2022).
- [43] C.-Y. Wang, Quantum echo in two-component Bose-Einstein condensates, *Phys. Rev. A* **109**, 063327 (2024).
- [44] V. Penna and A. Richaud, Two-species boson mixture on a ring: A group-theoretic approach to the quantum dynamics of low-energy excitations, *Phys. Rev. A* **96**, 053631 (2017).
- [45] A. Richaud and V. Penna, Quantum dynamics of bosons in a two-ring ladder: Dynamical algebra, vortexlike excitations, and currents, *Phys. Rev. A* **96**, 013620 (2017).
- [46] C. Charalambous, M. Á. García-March, G. Muñoz-Gil, P. R. Grzybowski, and M. Lewenstein, Control of anomalous diffusion of a Bose polaron, *Quantum* **4**, 232 (2020).
- [47] A. D. Cronin, J. Schmiedmayer, and D. E. Pritchard, Optics and interferometry with atoms and molecules, *Rev. Mod. Phys.* **81**, 1051 (2009).
- [48] H. Zhai, *Ultracold Atomic Physics* (Cambridge University Press, Cambridge, 2021).
- [49] K. Hasebe, $Sp(4; R)$ squeezing for Bloch four-hyperboloid via the non-compact Hopf map, *J. Phys. A: Math. Theor.* **53**, 055303 (2020).
- [50] E. V. Damaskinski, Calculation of Berry’s phase in squeezed states, *J Math Sci* **54**, 894 (1991).
- [51] O. Viyuela, A. Rivas, S. Gasparinetti, A. Wallraff, S. Filipp, and M. A. Martin-Delgado, Observation of topolog-

- ical Uhlmann phases with superconducting qubits, [npj Quantum Inf](#) **4**, 1 (2018).
- [52] M. Gabbrielli, L. Pezzè, and A. Smerzi, Spin-Mixing Interferometry with Bose-Einstein Condensates, [Phys. Rev. Lett.](#) **115**, 163002 (2015).
- [53] A. M. Marino, N. V. Corzo Trejo, and P. D. Lett, Effect of losses on the performance of an SU(1,1) interferometer, [Phys. Rev. A](#) **86**, 023844 (2012).
- [54] B. Yurke, S. L. McCall, and J. R. Klauder, SU(2) and SU(1,1) interferometers, [Phys. Rev. A](#) **33**, 4033 (1986).
- [55] C. J. Pethick and H. Smith, *Bose-Einstein Condensation in Dilute Gases*, 2nd ed. (Cambridge University Press, Cambridge, 2008).
- [56] S. Burger, K. Bongs, S. Dettmer, W. Ertmer, K. Sengstock, A. Sanpera, G. V. Shlyapnikov, and M. Lewenstein, Dark Solitons in Bose-Einstein Condensates, [Phys. Rev. Lett.](#) **83**, 5198 (1999).
- [57] J. Denschlag, J. E. Simsarian, D. L. Feder, C. W. Clark, L. A. Collins, J. Cubizolles, L. Deng, E. W. Hagley, K. Helmerson, W. P. Reinhardt, S. L. Rolston, B. I. Schneider, and W. D. Phillips, Generating Solitons by Phase Engineering of a Bose-Einstein Condensate, [Science](#) **287**, 97 (2000).